

# **DYNAMIC CHARACTERISTICS IDENTIFICATION FOR AN ARCH BRIDGE USING WIRELESS SENSOR NETWORKS BEFORE AND AFTER SEISMIC RETROFIT; THE APPLICATION TO MODEL UPDATING**

Tomonori Nagayama<sup>1</sup>

## **Abstract**

Functionalities of wireless sensors to measure bridge dynamic behavior are maturing; dense measurements of large structures are expected to reveal details of the behavior of existing structures. Traffic-induced vibrations at an arch bridge, instrumented by 48 wireless smart sensors, were measured before and after seismic retrofit of the structure. The differences between the measured dynamic characteristics represent the effects of seismic retrofit. A comparison of mode shapes reveals their changes, which are then used to update the finite element model of the bridge; densely measured mode shapes are also shown to be sensitive to structural changes. A potential use of dense instrumentation has been demonstrated.

## **Introduction**

Wireless Sensor Networks (WSN) are expected to serve as effective observation tools for condition evaluations of structures, leading to their more efficient management. WSN, which utilizes micro-electro-mechanical systems (MEMS) sensors and RF communication, is, in general, inexpensive and easy to install without the need for cabling. As basic functionalities to monitor structural dynamic behavior, such as synchronized sensing, loss-less multi-hop communication, and high resolution vibration measurement, have been proposed and prepared as middleware services, dense monitoring of structures using wireless sensors have become practical (Nagayama and Spencer 2007; Rice and Spencer 2009; Cho et al. 2010; Jang et al. 2010).

Multi-hop bulk data transfer proposed for data intensive applications (Nagayama et al 2010), in particular, made dense instrumentation of dynamic measurement sensors and analysis of collected data feasible. The application of the middleware service to a suspension bridge vibration monitoring revealed detailed mode shapes of the bridge, demonstrating practical usage of dense WSN in monitoring. However, the mode shapes were identified only at the measurement points located along one side of the main span girder and thus the analysis of the data has been restricted. For example, torsional motions were not distinguished from bending motions. The use of WSN did not result in detailed analysis of dynamic behaviors.

In this study, 48 wireless sensor nodes, programmed to synchronously sample

---

<sup>1</sup> Assistant Professor, Dept. of Civil Engineering, University of Tokyo, Tokyo

acceleration data which are then transported to the base station over multi-hop routes, are installed on the deck and ribs of an arch bridge, allowing its dynamic behaviors to be measured and analyzed. The measurements were performed both before and following a seismic retrofit so that the resultant changes in dynamic properties are analyzed. Finite element models created based on the design drawings of the bridge are then updated so that the natural frequencies and mode shapes identified from the obtained acceleration data as well as their changes are consistent with the eigenvalues and eigenvectors of the models. Finally, artificial damage was introduced on the model to study the sensitivity of dynamic properties to structural changes with particular emphasis on the densely measured mode shapes.

### **Wireless Sensor System**

The Imote2 is a smart sensor platform designed for data intensive applications (MEMSIC Corporation, 2012). The main board of the Imote2 incorporates a low-power X-scale processor, the PXA27x, and an 802.15.4 radio. The processor speed may be scaled based on application demands, thereby improving its power usage efficiency. One of the important characteristics of the Imote2 that separates it from previously developed wireless sensing nodes is the amount of data it can store and process. The Imote2 has 256 KB of integrated SRAM, 32 MB of external SDRAM, and 32 MB of Flash memory.

The SHM-A sensor board developed at the University of Illinois at Urbana-Champaign (Rice et al 2010), is employed. The sensor board provides user-selectable sampling rates and anti-aliasing filters for a broad range of applications. These functionalities are realized by the choice of appropriate key components such as the Quickfilter QF4A512 chip, which is an ADC and signal conditioner with programmable sampling rates and digital filters (Quickfilter Technologies, Inc. 2012), and the ST Microelectronics LIS344ALH capacitive-type MEMS accelerometer (STMicroelectronics 2012). The SHM-A board interfaces with the Imote2 via SPI I/O and has a three-axis analog accelerometer for vibration measurement. The noise levels of the tri-axis acceleration measurement have been experimentally determined to be 0.29 mg for the x- and y- axes and 0.67 mg for the z-axis in terms of their acceleration RMS levels when sampled at 50 Hz. With the low noise levels, traffic induced vibration of bridges are considered to be captured while the detectability of bridge ambient vibrations depends on the amplitude of ambient vibrations.

The software to operate the WSN is developed based on the Illinois SHM Project Tool suites (Rice et al 2010), a suite of services that implements on the TinyOS environment key middleware functionality to provide high-quality sensor data and to transfer the data reliably to the base station via wireless communication across the sensor network, and a library of numerical algorithms. Synchronized sensing is realized by employing the Flooding Time Synchronization algorithm (Maroti et al 2004) and resampling based on the global time stamps (Nagayama and Spencer 2007). This

open-source software is available at <http://shm.cs.uiuc.edu/software.html>. Upon the tool suites, customized services are implemented. Because deployment areas are usually large and does not always provide clear lines of sight between measurement nodes and the base station, AODV multi-hop routing protocol is implemented. Also, because the amount of data collected in bridge vibration measurement applications is much larger than other WSN applications and multi-hop communication is typically slow, packet collision avoidance utilizing multiple RF channels is leveraged to speed up the data collection.

Utilizing these functionalities, WSN was programmed to achieve the following processes. First, the routes from all of the measurement nodes to the two base station nodes are established. Then, time synchronization is performed and acceleration measurement starts. After sensing completes, post-processing is performed on each node to resample the data for accurate time synchronization among measurement data. All of the measurement nodes then start pushing their measurement data towards the base stations over the multi-hop routes using the multiple RF channel approach.



**Figure 1 THE IMOTE2 SENSOR NODES IN THE PLASTIC CASING**

As the original Imote2 development was for research purposes, this commercially available sensor node is not provided with rugged and water proof casing. The use of the Imote2 for bridge vibration measurement requires consideration on the practical aspects. To protect the Imote2 from the rain and dust, plastic casing is employed. The transparent lid allows users observe the Imote2 and its LED indicator. Instead of connecting the antenna directly to the Imote2, a co-axial elongation cable of one meter connects the antenna and the Imote2. As the sensor installation location is not necessarily at a location of a good RF communication condition, the elongation cable allows the installation of the antenna at better locations. In addition, the battery board holding three AAA batteries is replaced with a battery holder for two AA NiMH rechargeable batteries equipped with solar panels. The voltage regulator connected to the battery holder provides 5V supply to the Imote2. Though

the rechargeable batteries can be charged from the solar panels, available energy is not large enough to continuously operate the Imote2 and the regulator; the battery holder is used mainly to supply regulated voltage from fully-charged batteries to the Imote2. The customized casing, antenna, and battery holder are shown in Figure 1.

### **Object Bridge and Measurement**

The object bridge is an arch bridge in Iwate Prefecture along National Route 45 (see Figure 2). Seismic retrofit work conducted on this bridge added stiffening plates to the arch ribs and other vertical and horizontal members. As the result of the seismic retrofit, the dynamic characteristics changed. The horizontal vibration frequencies are expected to increase due to increase in stiffness. On the other hand, the vertical vibration frequencies are expected to decrease as the stiffness in vertical direction is large even before the retrofit, and the effects of the increase in mass are relatively large. The changes in other dynamic characteristics such as mode shapes and damping ratios are not easily predicted without building appropriate numerical models. To examine the change in dynamic properties due to the seismic retrofit, the bridge is instrumented with wireless smart sensor nodes (see Figure 3) and its traffic induced vibrations are measured and analyzed.



**Figure 2 THE OBJECT BRIDGE WHICH EXPERIENCED SEISMIC RETROFIT**

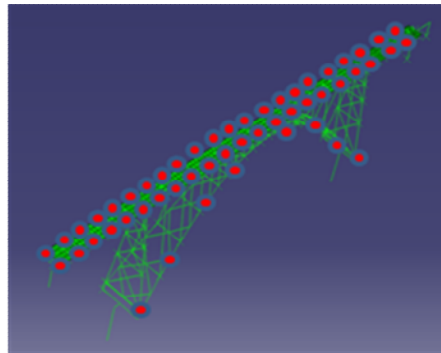


**Figure 3 THE INSTALLATION LOCATIONS OF 48 WIRELESS SMART SENSORS**

In total, 48 wireless smart sensors are installed on the bridge deck and the arch ribs. All of the sensor nodes are installed and removed on a daily basis. After about one hour of sensor installation, vibration measurements are repeatedly performed for about four hours. Then sensor removal of about one hour follows. These processes are repeated for two days for each of the before- and after-retrofit measurements. As the sensor has two axes with relatively lower measurement noise level, these two axes of the sensor nodes are set to the vertical and lateral directions. The other axis measures the longitudinal acceleration. Though acceleration is measured in all of the three directions, the vibration characteristics of the vertical and lateral modes are of the main interests. The sampling frequency is set as 50 Hz and measurement duration is six minutes. Data is collected from all of the nodes after each measurement, which takes about 20 minutes. In order to examine the validity of the WSN measurement data, six conventional wired servo-type tri-axis accelerometers (Tokyo Sokushin 2012) are installed on the deck. The installation locations of the six wired sensors are the same as those of six Imote2 nodes.

### **Identified Dynamic Properties**

The acceleration measurement data of the Imote2 nodes are first compared with those of the reference wired sensor nodes. When there is no traffic on the bridge and the vibration amplitude is small, the acceleration signals from the Imote2 sensor nodes are not large as compared to the noise level. However, traffic induced vibrations are at much larger amplitudes. Figure 4 shows the deck response signals recorded by an Imote2 node and a reference sensor node. The amplitude reaches 5 mg. The two signals show a good agreement in the time domain when the amplitude is large. Figure 5 shows the power spectral density estimation of the two signals. Several dominant frequency peaks are observable and the two power spectral density estimations are close to each other at the frequency ranges of the dominant frequencies. Frequency ranges of smaller amplitudes do not show a good correspondence.

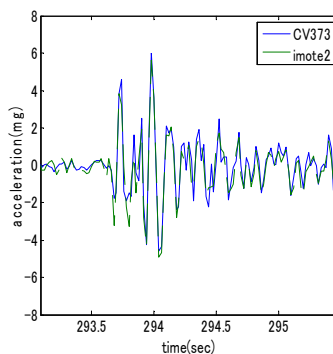


**Figure 4 VERTICAL ACCELERATION TIME HISTORY**

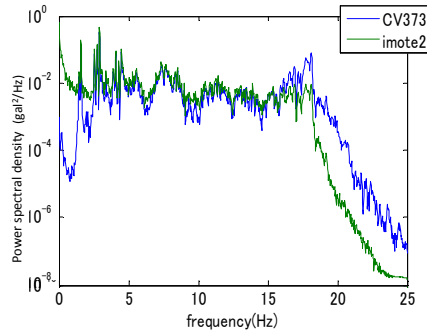


**Figure 5 VERTICAL ACCELERATION POWER SPECTRAL DENSITY ESTIMATION**

The peak-picking method is then employed to identify the vibration modes. Six modes in the vertical direction and five modes in the lateral directions are observed. The frequencies of these modes identified from the Imote2 and those from the reference nodes are almost the same; the difference is less than 1%. As for the mode shapes, Figure 6 shows the 1st vertical mode shape identified from the Imote2 nodes and the reference nodes on one side of the deck. Though the number of reference sensors is much less than that of the Imote2 nodes and comparison is only at limited locations, the mode shapes shows agreement. The agreement between the Imote2 and the reference sensor mode shapes are confirmed for other modes including lateral directions. However mode shapes identified from the arch rib sensor nodes did not result in reasonable mode shapes; a possible reason is that measurement data from sensors installed on the arch ribs inclined in both the longitudinal and lateral directions were not collectedly converted to the vertical and lateral directions.

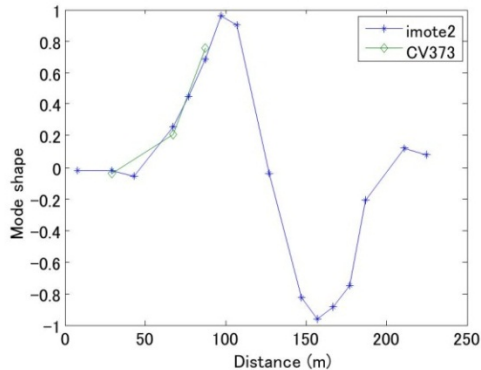


**Figure 6 COMPARISON OF 1<sup>ST</sup> VERTICAL MODE SHAPE IDENTIFIED FROM WIRELESS AND WIRED SYSTEM DATA SETS**

The identified modal properties before and after the seismic retrofit are then compared with each other. Table 1 shows the identified natural frequencies. The 1st vertical mode frequency does not change while the second vertical frequency decreases. On the other hand, the 1st and 2nd lateral frequencies both increase. As stated previously, the effect of increase in mass is considered dominant in the vertical modes and the effect of

increase in stiffness is considered dominant in the lateral modes. However the changes are not necessarily due only to the seismic retrofit. The change in environmental conditions such as temperature has been reported to affect the dynamic properties (Peeters et al. 2001; Farrar et al. 1997). The measurement before the retrofit is performed in March while the measurement after the retrofit was in September. The higher temperature after the seismic retrofit is a factor which potentially decreases the natural frequencies. Mode shapes changes are also observed. *Figure 7* Figure 7 shows the 1st vertical mode shapes identified from two measurements before the retrofit and two measurements after the seismic retrofit. The x-axis indicates the distance from the left-most joint. While the variation in the identified mode shapes are not negligible and the difference between the two mode shapes does not directly indicate mode shape changes, there are changes which distinguishes the two “before-retrofit” mode shapes from the two “after-retrofit” mode shapes. For example, the mode shape in the range of 70 m to 110 m shifts to the right after the retrofit. The changes are considered due to the seismic retrofit. Note that if the number of measurement points is small, the changes are difficult to detect. Even if change is detected, mode shape amplitude changes are difficult to distinguish from spatial shifts.

**Table 1 NATURAL FREQUENCIES IDENTIFIED FROM THE MEASUREMENT AND FEM**

	Measurement			FEM		
	before	after	change (%)	before	after	change (%)
Vertical 1st	1.44	1.44	0	1.4595	1.385	-5.1
Vertical 2nd	1.57	1.51	-3.8	1.566	1.448	-7.5
Lateral 1st	0.93	1.03	10.8	0.923	1.026	11.2
Lateral 2nd	1.58	1.66	5.1	1.616	1.669	3.3

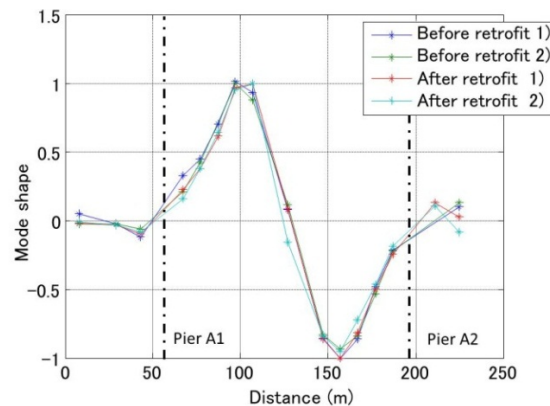


**Figure 7 1<sup>st</sup> VERTICAL MODE SHAPE**

### Comparison with Finite Element Models

Finite element models of the bridge before and after retrofit have been constructed based on the design drawing and their eigenvalues and eigenvectors are compared with modal properties identified from measurement. The commercial software, ABAQUS (Dassault Systemes 2012), is utilized in this analysis. The frequencies from measurement and FEM are summarized in Table 1. The identified natural frequencies in the lateral direction show agreement with those of FEM. On the other hand, the identified frequency changes of the vertical modes are smaller than those of FEM. As for mode shape changes, there are changes observable both in measurement and FEM as well as changes observed only in one of them. For example, the mode shape shift of the identified 1st vertical mode to the right in the range of 70 m to 110 m is observed in FEM as well. However the shift is too large as compared to the shift observed in the measurement.

As the vertical natural frequencies of the FEM are higher than identified frequencies, the FEM is considered to have smaller stiffness in vertical direction than the structure. Assuming that the difference between the boundary condition of the model and the bridge is the main source of the modal property difference, the boundary conditions are updated. Even when bearings of bridges are designed to freely rotate or slide, the bearings oftentimes do not move under small load. As the studied arch bridge is under small traffic load, there is a possibility that the behavior of bearings is similar to fixed boundary condition. Each bearing is assumed either fixed or movable and eigenvalues and eigenvectors are calculated. All combinations of bearing conditions are examined to choose the bearing condition which produces modal properties consistent with identified properties. When the rotation of the bearing at 57 m from the left is assumed fixed, the frequencies and mode shapes became closest to the identified modal properties. Table 2 lists the natural frequencies after the boundary condition update. Figure 8 illustrates the mode shapes after the update. The mode shape shift to the right in the range of 70 m to 110 m becomes closer to the shift observed in the measurement.

**Table 2 NATURAL FREQUENCIES BEFORE AND AFTER THE MODEL UPDATE**

After seismic retrofit	FEM before update	FEM after update	measurement
Vertical 1st	1.385	1.402	1.44
Vertical 2nd	1.448	1.533	1.51

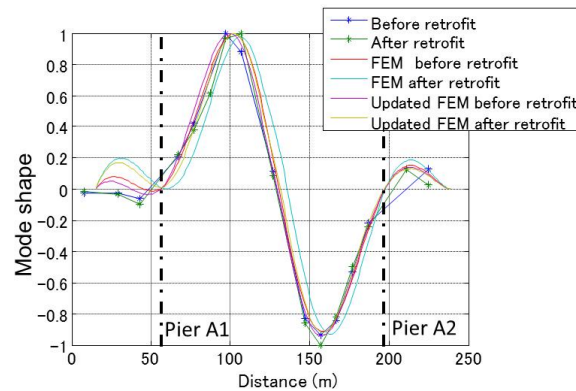


**Figure 8 1<sup>ST</sup> VERTICAL MODE SHAPES BEFORE AND AFTER THE MODEL UPDATE**

### **Sensitivity of Mode Shapes to Structural Damages**

A sensitivity analysis of modal properties with respect to structural damages is performed. As modal properties have been reported not to be sensitive to structural damages (Farrar et al 1997), evaluating structural condition through vibration measurement is considered difficult. Modal frequencies do not change at a large amount even when bridge structural members experience damages. Furthermore, frequencies are reported to be sensitive to environmental parameters such as temperature. However, the sensitivity of densely measured mode shapes of bridges has not been studied intensively. Using the finite element model of the objective bridge, two types of damages are introduced and the resultant mode shape changes are examined. As possible damages to the arch bridge, element cut at the crown point of the arch rib due to fatigue and cross sectional loss of arch rib bottom part are separately considered. Mode shapes sensitive to structural change can possibly be used in structural condition assessment.

When one element at the crown point of the arch rib is removed assuming severe fatigue crack, modal frequency changes are 0 %, 0 %, 1 %, and 2 % for 1<sup>st</sup> transverse mode, 2<sup>nd</sup> transverse mode, 1<sup>st</sup> vertical mode, and 2<sup>nd</sup> vertical mode. While the transverse mode shapes do not show clear changes, the vertical mode shapes exhibits differences. Figure 9 shows the 1<sup>st</sup> vertical mode shapes of the arch rib. The difference is clear. Change of similar degree has been observed for the 2<sup>nd</sup> vertical mode shape. Even when the mode frequency changes are small, the corresponding mode shape changes are large. Dense measurement of bridges can possibly detect these mode shape changes.

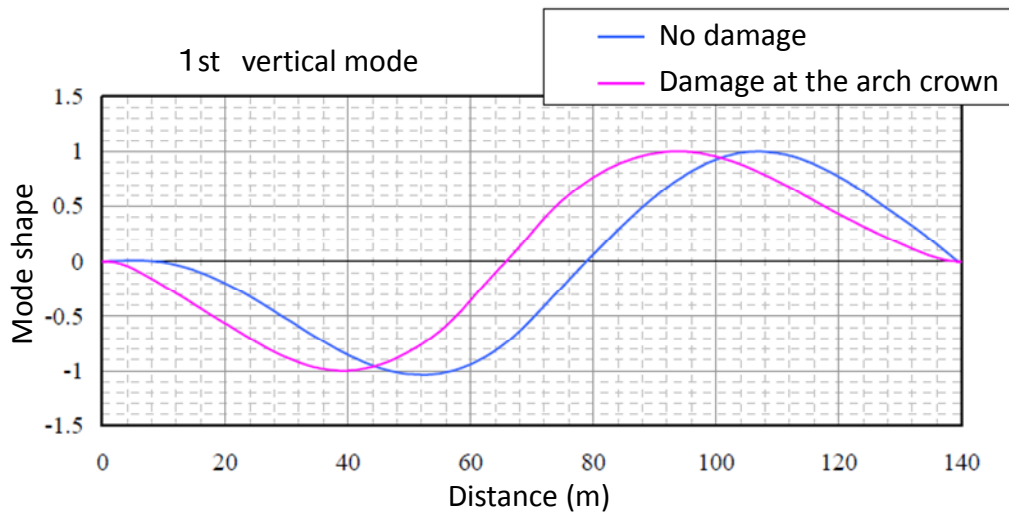


**Figure 9 1<sup>st</sup> vertical mode with damage at the crown point of the arch**

When four bottom parts of the arch ribs experience cross sectional loss of 75 % assuming severe corrosion, modal frequency changes are 12%, 4%, 3%, and 5% for 1<sup>st</sup> transverse mode, 2<sup>nd</sup> transverse mode, 1<sup>st</sup> vertical mode, and 2<sup>nd</sup> vertical mode. The frequency changes are large as the assumed damage is severe. Figure 10 shows the 1<sup>st</sup> vertical mode shapes of the arch rib. Change of similar degree has been observed for the 2<sup>nd</sup> vertical mode shape.

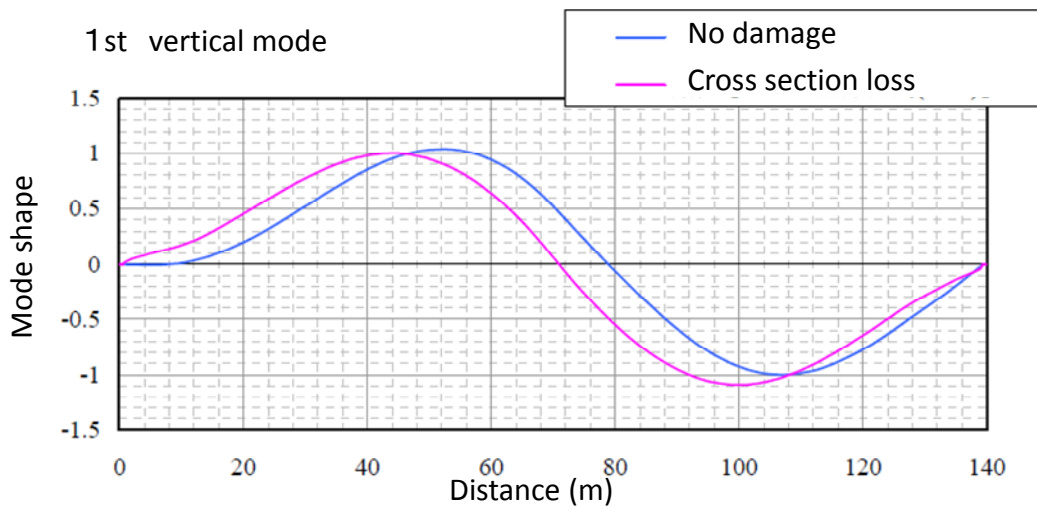


**Figure 10 1<sup>st</sup> vertical mode with cross section loss at the arch base**

## Conclusion

An arch bridge was instrumented with 48 wireless smart sensors and its dynamic

behavior was captured in detail. Modal properties have been identified from the measurement and their comparison with FE models revealed the differences in the modal properties. Mode shapes in addition to natural frequencies were used to update the FE model boundary conditions. Though the FE models and modal identification errors need further consideration, this study demonstrates the use of dense measurement and its resultant detailed mode shapes in updating the FE model.

### **Acknowledgments**

The author gratefully acknowledges the partial support of this research by the Japan Society for the Promotion of Science Grant-in-Aid for Young Scientists (B) (20760298), the Japan Institute of Construction Engineering research grant, and Japan Steel Bridge Engineering Association.

### **References**

Cho S., Jo, H., Jang, S.A., Park, J., Jung, H.J., Yun, C.B., Spencer, Jr., B.F., and Seo, J.W., "Structural health monitoring of a cable-stayed bridge using wireless smart sensor technology: data analyses," *Journal of Smart Structures and Systems*, 6(5), 461-480 (2010).

Dassault Systemes, <<http://www.3ds.com/products/simulia/portfolio/abaqus/overview/>> (Sep. 1, 2012).

Farrar, C.R., Doebling, S.W., Cornwell, P.J., Straser, E.G., "Variability of modal parameters measured on the Alamosa Canyon Bridge," *Proc. IMAC 15, Orlando, FL, USA*, 257-263 (1997).

Jang, S.A., Jo, H., Cho, S., Mechitov, K.A., Rice, J.A., Sim, S.H., Jung, H.J., Yun, C.B., Spencer, Jr., B.F., and Agha, G., "Structural Health Monitoring of a Cable-stayed Bridge using Smart Sensor Technology: Deployment and Evaluation," *Journal of Smart Structures and Systems*, 6(5), 439-459 (2010).

Maróti, M., Kusy, B., Simon, G. and Lédeczi, A., "The flooding time synchronization protocol", *Proc. the 2nd International Conference on Embedded Network Systems*, Baltimore, Maryland, USA, November (2004).

MEMSIC Corporation, <<http://www.memsic.com>> (Sep. 1, 2012).

Nagayama, T., and Spencer Jr., B. F., "Structural Health Monitoring using Smart Sensors," *NSEL Report Series, No. 1, University of Illinois at Urbana-Champaign* (2007).  
<http://hdl.handle.net/2142/3521>.

Nagayama, T., Moizadeh, P., Mechitov, K., Ushita, M., Makihata, N., Ieiri, M., Agha, G., Spencer Jr., B. F., Fujino, Y., Seo, J., "Reliable multi-hop communication for structural health monitoring," *Smart Structures and Systems*, 6(5), 481-504 (2010).

Peeters, P., Maeck, J., and Roeck, G.D., "Vibration-based damage detection in civil

engineering: excitation sources and temperature effects,” *Smart Materials and Structures*, 10(3), 518-527 (2001).

Quickfilter Technologies, Inc., < <http://www.quickfiltertech.com/> > (Sep. 1, 2012).

Rice, J. A. and Spencer Jr., B. F. “Flexible Smart Sensor Framework for Autonomous Full-scale Structural Health Monitoring,” NSEL Report Series, No. 18, University of Illinois at Urbana-Champaign (2009). <http://hdl.handle.net/2142/13635>.

Rice, J. A., Mechitov, K., Sim, S. H., Nagayama, T., Jang, S., Kim, R., Spencer Jr., B. F., Agha, G. and Fujino, Y., “Flexible Smart Sensor Framework for Autonomous Structural Health Monitoring,” *Smart Structures and Systems*, 6(5), 423-438 (2010).

STMicroelectronics, < <http://www.st.com/>> (Sep. 1, 2012).

Tokyo Sokushin, < <http://www.to-soku.co.jp/>> (Sep. 1, 2012).